

## Supplementary information

### Supplementary tables

**Table S1:** Statistical analysis for Ki67 and BrdU cell numbers in Fig. 2 (G) and (H).

**Table S2:** ANOVA analysis of probe tests of MWM in Fig. 2 (C-D) and Fig. 3 (D-G).

### Supplementary figure legends

**Figure S1.** The expression of the Nestin-tk transgene in multiple tissues and the effect of the GCV treatment on neural progenitor proliferation in wildtype mice. **(A)** The expression of the Nestin-tk transgene in six different tissues. RT-PCR only detected the transgene expression in the brain but not other tissues. H<sub>2</sub>O was used as negative control and plasmid was used as positive control. **(B-D)** The GCV treatment does not affect progenitor cell proliferation in wildtype mice. **(B)** The experimental scheme. **(C)** Representative images showing the BrdU-labeled neural progenitor cells in SGZ of the dentate gyrus in GCV- and vehicle-treated C56BL/6 mice. **(D)** Quantification of the number of BrdU cells in SGZ revealed no significant difference between the GCV- and vehicle-treated wildtype mice ( $t_8=0.355$ ,  $p>0.73$ ;  $n=5$  for each group). Error bars represent  $\pm$  sem.

**Figure S2.** Reduced cell proliferation in the SGZ and the SVZ of Nestin-tk mice after four days of the GCV treatment. **(A)** The experimental scheme. **(B-G)** Representative images showing the decreased progenitor cell proliferation in tg-GCV in both the SGZ of the dentate gyrus **(B-E)** and the SVZ of the lateral ventricle **(F and G)** using BrdU **(B, C, F, G)** and Ki67 (red and arrows, **D and E**) as markers. DAPI (green) marks all cell nuclei in **D and E**. **(H)** Quantification of the number of BrdU cells in the SGZ, which is significantly reduced in tg-GCV mice (ANOVA,  $F_2$ ,

$t_{41}=20.62$ ,  $p<6\times 10^{-7}$ ; for wt-GCV,  $n=16$ ; for tg-GCV,  $n=17$ ; for tg-PBS,  $n=11$ ). **(I)** Quantification of the number of Ki67 cells in the SGZ, which is significantly reduced in tg-GCV mice (ANOVA,  $F_{2,7}=16.27$ ,  $p<0.002$ ; for wt-GCV,  $n=3$ ; for tg-GCV,  $n=3$ ; for tg-PBS,  $n=4$ ). **(J)** Quantification of the number of BrdU cells in the SVZ, which is significantly reduced in tg-GCV mice ( $t_9=4.68$ ,  $p<0.0011$ ; for wt-GCV,  $n=6$ ; for tg-GCV,  $n=5$ ). Four sections that contained lateral ventricles and were 240  $\mu\text{m}$  apart from each other were used for quantification. The bar in **B** represents 200  $\mu\text{m}$  for **B** and **C** and represents 80  $\mu\text{m}$  for **D** and **E**. \* indicates statistically significant difference. Error bars represent  $\pm$  sem.

**Figure S3.** Gliogenesis is not affected by GCV treatment in Nestin-tk mice. **(A)** The experimental scheme. **(B-C)** Representative images of BrdU (red), GFAP (green) double-positive cells (arrows) in wt-GCV **(B)** and tg-GCV **(C)** mice. **(D-E)** Neurogenesis but not gliogenesis is affected by GCV treatment in Nestin-tk mice. **(D)** Quantification of the number of BrdU/GFAP double-positive cells in the dentate gyrus. There is no reduction in the number of double-labeled cells in tg-GCV mice ( $t_9=0.342$ ,  $p>0.740$ ;  $n=5$  for wt-GCV;  $n=6$  for tg-GCV). **(E)** Quantification of the number of BrdU/NeuN double-positive cells in the dentate gyrus, showing the reduction in the tg-GCV mice ( $t_9=3.57$ ,  $p<0.006$ ). \* indicates statistically significant difference. Error bars represent  $\pm$  sem.

**Figure S4.** Reduction of adult neurogenesis in another two lines of GCV-treated Nestin-tk transgenic mice. **(A-B)** Cell proliferation labeled by BrdU **(A)**, ANOVA,  $F_{2,28}=42.90$ ,  $p<3\times 10^{-9}$ ; for wt-GCV,  $n=10$ ; for tg-GCV,  $n=12$ ; for tg-Veh,  $n=9$ ) and immature neurons labeled by Dcx **(B)**, ANOVA,  $F_{2,28}=183.06$ ,  $p<8\times 10^{-17}$ ) are both reduced in line 1920 of Nestin-tk transgenic

mice treated with GCV. **(C-D)** Cell proliferation labeled by BrdU **(C)** and immature neurons labeled by Dcx **(D)** are both reduced in line 1918 of Nestin-tk transgenic mice treated with GCV (n=2 in each group). \* indicates statistically significant difference. Error bars represent  $\pm$  sem.

**Figure S5.** GCV treatment does not cause body weight changes or inflammation in transgenic mice. **(A-B)** Body weight changes in animals treated with GCV for 4 days **(A)**, ANOVA,  $F_{2,41}=1.13$ ,  $p>0.33$ ; for wt-GCV, n=16; for tg-GCV, n=17; for tg-PBS, n=11) or 14 days **(B)**, ANOVA,  $F_{2,21}=0.70$ ,  $p>0.50$ , n=8 for each group). **(C-D)** Body weights of tg-GCV mice are not significantly different from those of wt-GCV mice or tg-Veh mice either before **(C)**, ANOVA,  $F_{2,21}=0.30$ ,  $p>0.74$ ) or after **(D)**, ANOVA,  $F_{2,21}=0.72$ ,  $p>0.50$ ) treatment with GCV for 14 days. **(E-F)** There is no detectable inflammation caused by GCV treatment in transgenic mice. The numbers of macroglia labeled by CD68 **(E)**,  $t_{12}=1.209$ ,  $p>0.24$ ; n=7 for each group) and Ox42 **(F)**,  $t_{12}=0.644$ ,  $p>0.53$ ; n=7 for each group) are similar in tg-GCV and wt-GCV groups. Error bars represent  $\pm$  sem.

**Figure S6.** Neurogenesis is reduced in three cohorts of mice on the standard hidden platform version of MWM, as indicated by the numbers of BrdU-labeled cells measured during the last four days of GCV treatment. **(A)** The 1-week delay cohort ( $t_{17}=3.499$ ,  $p<0.003$ ; for wt-GCV, n=10; for tg-GCV, n=9). **(B)** The 3.5-week delay cohort ( $t_{16}=8.608$ ,  $p<3\times 10^{-7}$ ; for wt-GCV, n=9; for tg-GCV, n=9). **(C)** The 9-week delay cohort ( $t_{22}=10.930$ ,  $p<3\times 10^{-10}$ ; for wt-GCV, n=13; for tg-GCV, n=11). \* indicates statistically significant difference. Error bars represent  $\pm$  sem.

Supplementary table 1: Statistical analysis for Ki67 and BrdU cell numbers in Fig. 2 (G) and (H)

	1 week delay	3 week delay	9 week delay
wt-GCV	n=7	n=5	n=10
tg-GCV	n=7	n=7	n=8
Ki67	$t_{12}=0.778, p > 0.44$	$t_{10}=0.809, p > 0.43$	$t_{16}=1.004, p > 0.33$
BrdU	$t_{12}=3.315, p < 6 \times 10^{-3}$	$t_{10}=3.228, p < 9 \times 10^{-3}$	$t_{16}=5.519, p < 4 \times 10^{-5}$

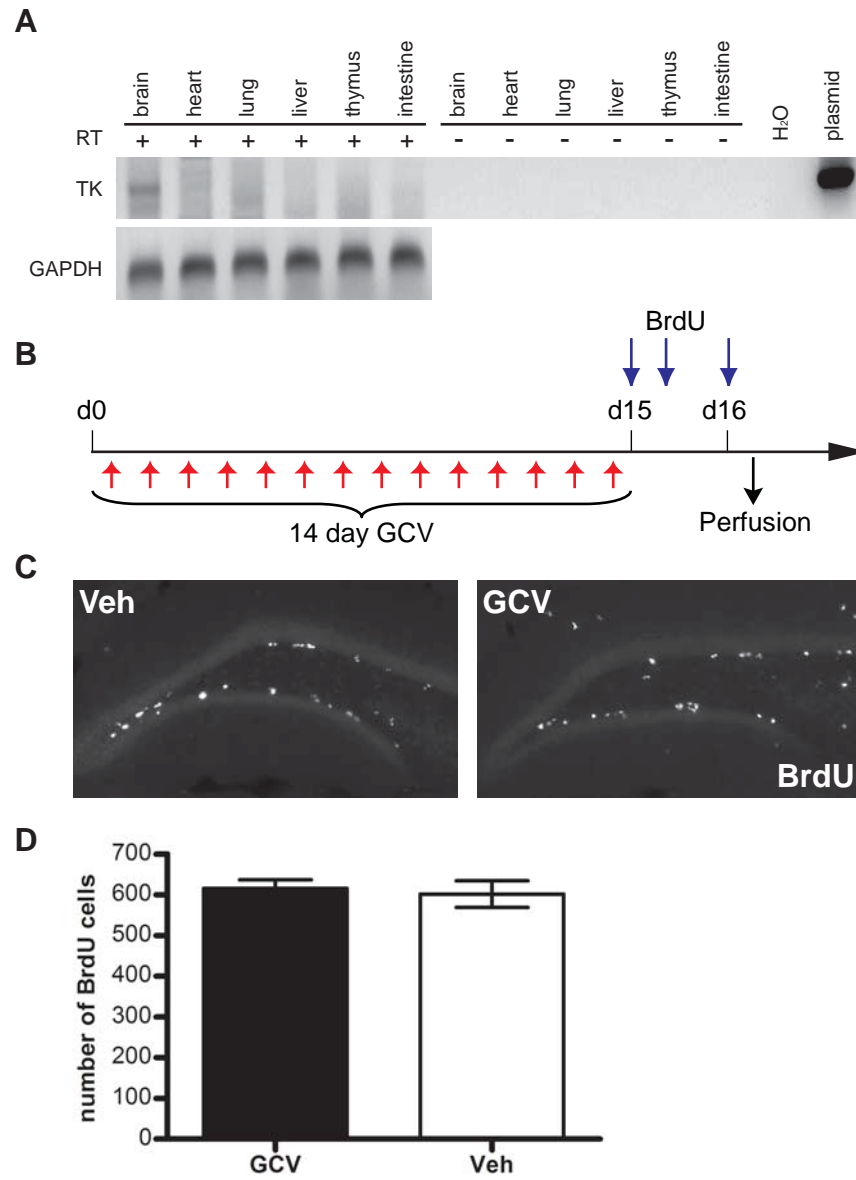
Supplementary table 2: ANOVA analysis of probe tests of MWM in Fig. 3 (C-D) and Fig. 4 (D-G).

	1-week delay cohort				3.5-week delay cohort				9-week delay cohort			
	wt-GCV		tg-GCV		wt-GCV		tg-GCV		wt-GCV		tg-GCV	
	$F_{3,60}$	p	$F_{3,60}$	p	$F_{3,32}$	p	$F_{3,36}$	p	$F_{3,48}$	p	$F_{3,40}$	p
day 4	4.930	0.0040	7.438	0.0030	3.141	0.0387*	5.096	0.0048	3.147	0.0334*	6.911	0.0007
day 5	4.969	0.0038	14.234	0.0001	6.371	0.0016	6.313	0.0015	6.495	0.0009	4.491	0.0083
day 6	8.873	0.0001	5.653	0.0018	6.605	0.0022	9.015	0.0001	5.815	0.0018	14.585	0.0001
day 7	11.342	0.0001	4.961	0.0038*	9.710	0.0001	7.695	0.0004	13.836	0.0001	27.346	0.0001
day 8	14.219	0.0001	3.123	0.0324*	10.882	0.0001	16.952	0.0001	7.658	0.0003	7.709	0.0004
week 1	7.567	0.0002	2.256	0.0911	24.218	0.0001 <sup>#</sup>	8.527	0.0003	10.581	0.0001	9.550	0.0001

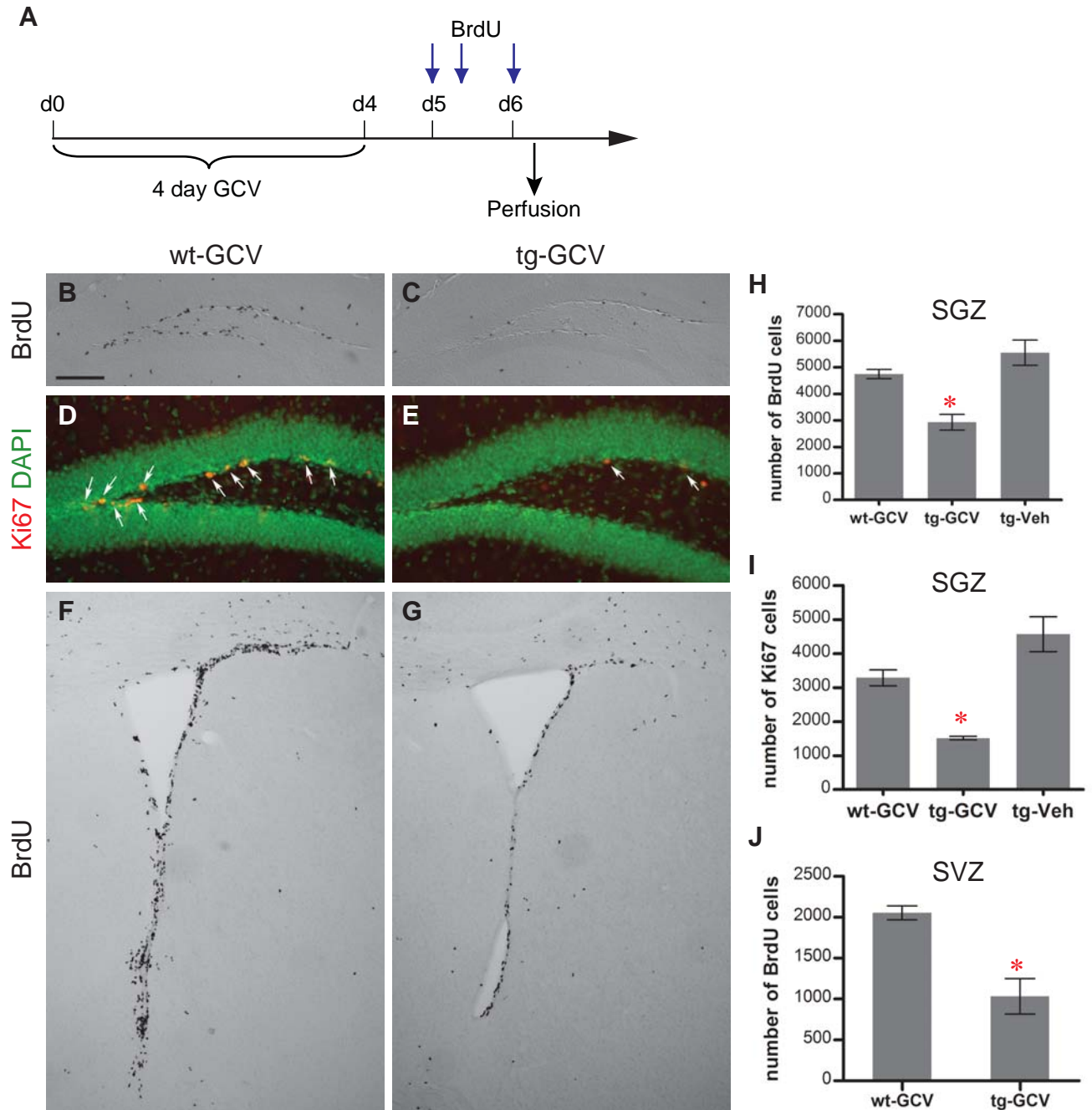
\*: post hoc test suggests that time spent in the target quadrant is not significantly more than at least one other quadrant.

#: time spent in the target quadrant is significantly above chance but not significantly more than one other quadrant.

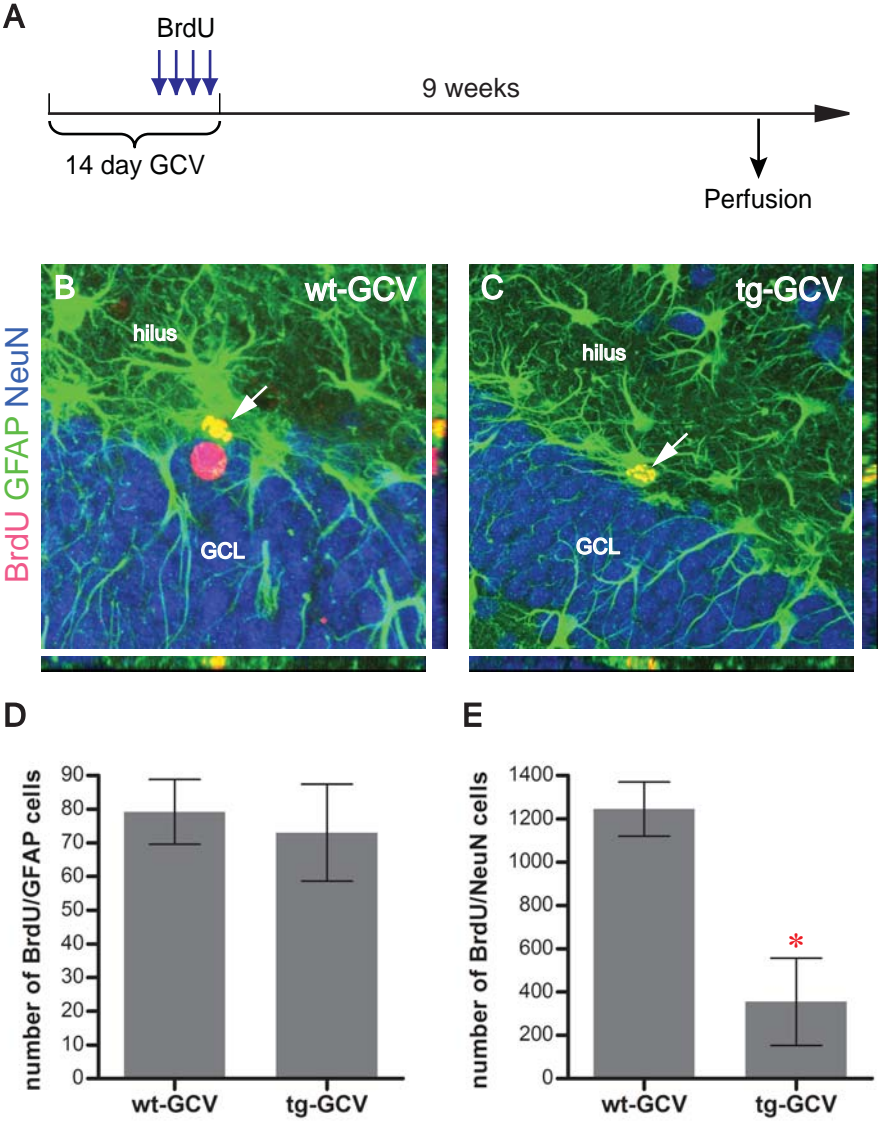
Supplementary figure 1, Deng et al.



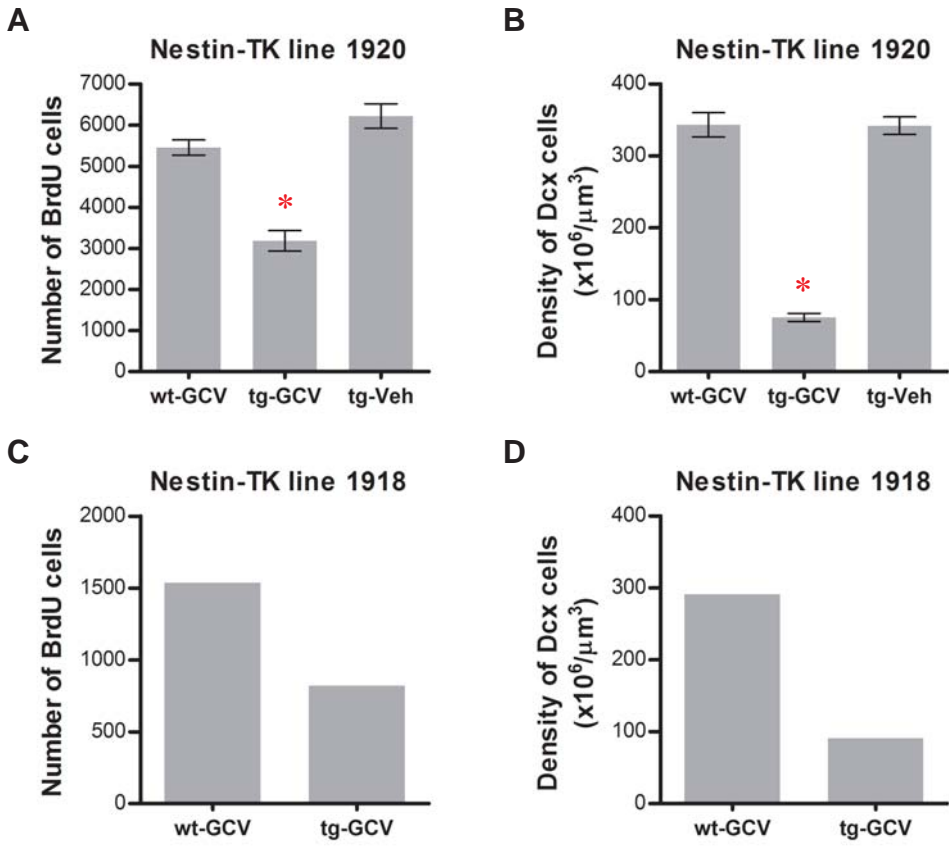
Supplementary figure 2, Deng et al.



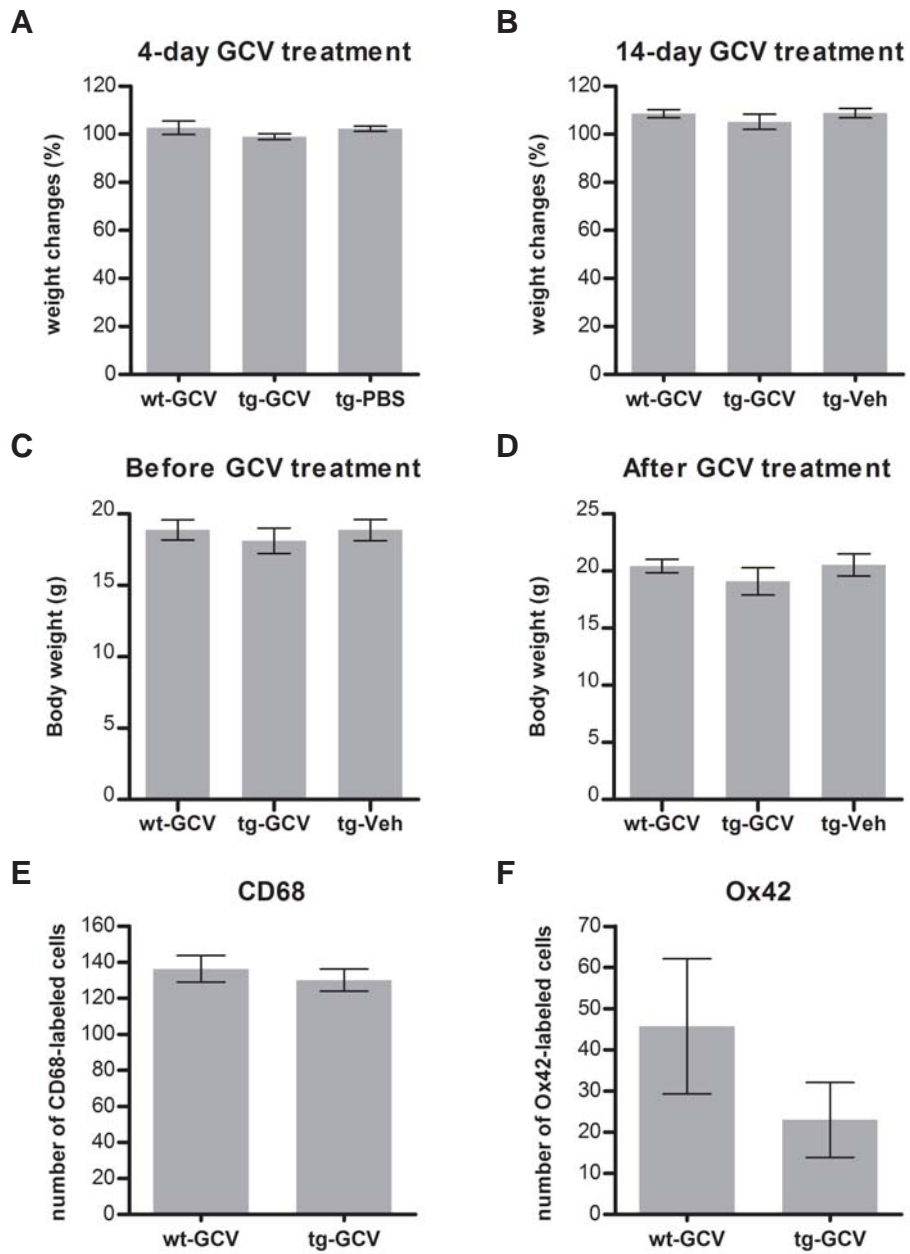
Supplementary figure 3, Deng et al.



Supplementary figure 4, Deng et al.



Supplementary figure 5, Deng et al.



Supplementary figure 6, Deng et al.

